

Excited Electronic States of the Cyclic Isomers of O₃ and SO₂

Ruth Elliott, Ryan Compton, Robert Levis, and Spiridoula Matsika*

Department of Chemistry and Center for Advanced Photonics Research, Temple University, Philadelphia, Pennsylvania 19122

Received: August 9, 2005

The low-lying electronic states of O₃ and SO₂ in their bent and cyclic isomers up to about 10 eV are calculated using the multireference configuration interaction (MRCI) method with a standard Gaussian correlation consistent polarized triple- ζ (cc-pVTZ) basis set. The vertical excitation energies, electron configurations, and oscillator strengths of these states are reported. The molecular orbital structures and excited states of the cyclic isomers are discussed in relation to the bent ones. Coherent anti-Stokes Raman spectroscopy (CARS) schemes for detecting the synthesis of the cyclic isomers are suggested.

Introduction

After the discovery of ozone by Schönbein in 1840, Meyer reasoned that O₃ was cyclic on the basis of early valence theory.¹ While there has been ongoing interest in producing the cyclic form of O₃, spectroscopic investigations have revealed that the true structure of ozone was acyclic and nonlinear.^{2,3} In fact, we have been unable to find reports of the synthesis or observation of the cyclic isomer for free O₃ or the isoelectronic SO₂ or S₃. However, Plass et al. have observed evidence for *cyclic*-O₃ on a MgO surface.⁴ Also, *cyclic*-S₂O has been synthesized by irradiating SSO isolated in a solid Ar matrix with light at 308 nm using a XeCl excimer laser.^{5,6} A new approach to synthesizing *cyclic*-O₃ using strong laser fields and the detection of *cyclic*-O₃ is under investigation and motivates the present calculations of the excited-state structure of cyclic triatomic molecules.

Using ab-initio calculations, *cyclic*-O₃ was proposed as a stable chemical species by Peyerimhoff and Buenker in 1967.⁷ Theoretical studies regarding the stability of *cyclic*-O₃ have been reported since the mid seventies, and many researchers have calculated energetics for the *cyclic*-O₃ minima, the ozone minima, and the O + O₂ dissociation barrier.^{8–21} Using the coupled cluster model of electron correlation with single and double excitations and perturbative triples (CCSD(T)) and an atomic natural orbital basis set, Lee found that the ground state of *cyclic*-O₃ lies 29.1 kcal/mol¹⁰ above the ground state for ozone and slightly above the experimental dissociation energy for O₃ → O₂ + O of 26.1 kcal/mol.²² Using the multireference configuration interaction (MRCI) level of theory and a correlation consistent polarized valence quadruple- ζ (cc-pVQZ) basis set, Siebert et al. calculated this value to be 30.9 kcal/mol.¹⁶ The barrier to forming *cyclic*-O₃ from bent O₃ was calculated by the same authors to be 54.7 kcal/mol.¹⁶ Müller et al. calculated the energy difference range to be 29.1 to 32.2 kcal/mol using the CCSD(T), MRCI, and MR-AQCC levels of theory and the estimated complete basis set limits for CCSD(T) and MR-AQCC levels.⁹ Many other theoretical investigations have explored the potential energy surface of the ground state of ozone and have largely confirmed these energetics.^{13–15,17–21}

While there appear to be no reports of the synthesis of free *cyclic*-O₃ to date, there is much evidence that creating the cyclic

isomer should be possible. The ground state of *cyclic*-O₃ has been studied extensively as it is a local minimum on the ground-state potential energy surface of ozone.^{9,10,12,15,18,23} *Cyclic*-O₃ is expected to be stable, once formed, because of the electronic structure of the isomer. The barrier to ring-opening is high (23.5 kcal/mol).¹⁶ Atchity et al. suggested that direct dissociation to O₂ + O occurs only through the open minima.¹⁵ In comparison with bent ozone, *cyclic*-O₃ has one additional π -electron pair and one less σ -electron pair. As has been stated before, this leads to an orbital-symmetry forbidden reaction back to ozone (or to O₂ + O) once *cyclic*-O₃ is formed.²⁴ Flemmig et al., using the calculated activation barrier and an estimated preexponential factor for the ring-opening reaction, predicted the room-temperature lifetime of *cyclic*-O₃ to be around 30 s, with much longer lifetimes at lower temperatures.²⁴ The difficulty in forming *cyclic*-O₃ in the gas phase is presumably due to the decomposition path to O + O₂ which has a lower barrier (26.1 kcal/mol)²² in comparison to the barrier to *cyclic*-O₃ formation (54.7 kcal/mol).^{16,25} Once *cyclic*-O₃ is formed, the stabilization and detection of the isomer seems possible. The stabilization of *cyclic*-O₃ with transition metals has been studied by Flemmig et al. using density functional theory (DFT).²⁴ From their calculations, Flemmig et al. propose using transition metal complexes to bind *cyclic*-O₃; they found that d⁶ or d⁸ transition metals with nitrosyl ligands form stable minimum complexes with *cyclic*-O₃ and *cyclic*-S₃. Siebert et al. have explored the vibrational spectrum of *cyclic*-O₃, finding it much different from that of O₃;²⁶ this fact may allow differentiation of O₃ and *cyclic*-O₃ spectroscopically.

The electronic structure of ozone has been investigated intensively. The vertical excitation energies, electron configurations, optimal geometries, and potential energy curves for the ground state of ozone and the next eight excited states have been studied.^{11,13,14,18,27,28} Banichevich et al. have calculated the potential energy curves of the excited states of ozone,^{13,14} but the details regarding the excited states at the cyclic geometry have not been reported to the best of our knowledge.

Likewise, free *cyclic*-SO₂ has not yet been created or isolated. The minimum energy geometry is bent, but the existence of a low-lying SO₂ isomer was first suggested as an explanation for the strong continuous absorption band which resulted from flash-initiated explosions of H₂S, CS₂, and COS.^{29–31} Assuming that

* Corresponding author. E-mail: smatsika@temple.edu.

the molecule responsible for the absorption band was a direct precursor to SO₂, many investigated the possibility of a superoxide (S–O–O) isomer.^{29,32,33} Influenced by the studies of Shih et al.⁸ on *cyclic*-O₃, the possibility of a low-lying ring isomer of SO₂ began to be investigated.^{23,34–37} Kellogg et al. found that all three SO₂ isomers were minima at the MRCI level of theory.³⁶ While the energy difference between O₃ and *cyclic*-O₃ is on the order of 30 kcal/mol, the difference between the open and ring isomers of SO₂ is calculated to be around 100 kcal/mol. Kellogg et al. calculated the difference to be 104 kcal/mol, using the CCSD(T) level of theory and triple- ζ plus double polarization f-type functions.³⁶ Ivanic et al. reported a difference of 97.2 kcal/mol, using the full optimized reference space (FORS) level of theory, which is equivalent to the complete active space self-consistent field method (CASSCF), and a cc-pVTZ basis set.²³ The large difference between the energy differences of the SO₂ and O₃ isomers is probably due to the increased stability of the O–SO bond in open SO₂ as compared to the O–OO bond in ozone.³⁵ This is indicated by the high dissociation limit of SO₂ into SO and O, which is 132 kcal/mol,³⁸ and the lower limit for ozone, which is 26.1 kcal/mol. Theory predicts a high barrier to ring-closing because of the σ – π electron transition, which is similar to that found in the ring-closing of O₃.^{23,35} In 1997, Ivanic et al. found the transition state energy of ring-closing to be 113 kcal/mol above the global minimum, using a state-averaged multi-configurational self-consistent field (MCSCF) calculation. As opposed to O₃, the ring-closing energy is lower than the dissociation limit. Once *cyclic*-SO₂ is formed, the barrier to ring-opening is predicted to be 15.6 kcal/mol,²³ much smaller than that of O₃. Consequently, the lifetime of *cyclic*-SO₂ predicted from the ring-opening barrier and an estimated preexponential factor of 10¹⁵/s is approximately 275 μ s at room temperature.

Many other calculations of the SO₂ ground-state potential energy surface have been reported.^{39–45} Excited-state potential energy surfaces have been studied by Kamiya et al.⁴⁵ Although the vertical excitation energies of SO₂ have been reported,^{28,46–48} details on the vertical excitations in the cyclic form of SO₂ have not been reported to the best of our knowledge.

A number of factors motivate the present investigation of the electronic states of *cyclic*-O₃ and *cyclic*-SO₂. An effort is underway to synthesize *cyclic*-O₃ using strong-field, shaped laser pulses.⁴⁹ Detailed knowledge of the excited electronic structure will facilitate design of the appropriate laser pulse shape for synthesis of *cyclic*-O₃ using photonic reagents.⁵⁰ For example, excited-state information will be necessary to perform time-dependent calculations for initial laser pulse shapes that may be required to determine the optimal pulse shapes in the feedback experiment.⁵⁰ During the optimization of the photonic reagent in current experiments, some feedback signal is required. Mass spectrometry cannot be employed to detect *cyclic*-O₃ because the mass-to-charge ratio is identical to that for bent ozone. The current experimental effort relies on the use of coherent anti-Stokes Raman spectroscopy (CARS) to detect the formation of *cyclic*-O₃. To employ CARS, knowledge of the excited-state electronic energies is necessary. Last, absorption spectroscopy is another possibility for detection of O₃ and *cyclic*-O₃, but again, some knowledge of the electronic excited states is essential. Here we report the energies corresponding to the ground and first several electronic states of bent and *cyclic*-O₃ and bent and *cyclic*-SO₂. Theoretically, SO₂ is of interest as isovalence model for the cyclization of triatomic molecules.

TABLE 1: Geometries Used in MRCI Calculations

species	bond angle (°)	bond length (Å)
O ₃ ^a	Θ_{OOO} 116.8	r_{OO} 1.272
<i>cyclic</i> -O ₃ ^b	Θ_{OOO} 60	r_{OO} 1.437
SO ₂ ^c	Θ_{OSO} 119	r_{SO} 1.432
<i>cyclic</i> -SO ₂ ^d	Θ_{OSO} 52.17 Θ_{SOO} 64	r_{SO} 1.65 r_{OO} 1.451

^a Ref 3. ^b Ref 9. ^c Ref 57. ^d Ref 36.

Experimentally, SO₂ is readily available as a stable gas-phase species and may present a useful model for cyclizing triatomic molecules.

Methods

The calculations were performed at the MRCI level of theory using the COLUMBUS suite of programs.⁵¹ The cc-pVTZ basis sets were used with the contractions (10s5p2d1f)/[4s3p2d1f] for oxygen⁵² and (15s9p2d1f)/[5s4p2d1f] for sulfur.⁵³ Both pairs of isomers were studied using C_{2v} symmetry. For *cyclic*-O₃, the results are reported using D_{3h} symmetry as well to clarify the discussion. For ozone, the orbitals were obtained from an average of states CASSCF with a complete active space of 12 electrons in 9 valence orbitals (CAS (12/9)). The nine 2p orbitals of oxygen were in the active space, and this active space generated 666, 614, 626, and 614 references for ¹A₁, ¹B₁, ¹B₂, and ¹A₂ symmetries, and 831, 855, 861, and 855 references for the ³A₁, ³B₁, ³B₂, and ³A₂ symmetries, respectively. The states averaged were those under consideration. At the MRCI level, the references were the same, the three 1s orbitals were frozen as the core, and the 2s orbitals and the CAS were correlated using single and double excitations. This calculation corresponded to about 39 million configurations for every irreducible representation of multiplicity 1 and about 64 million for every irreducible representation of multiplicity 3. Only the references that have the same symmetry as the states under investigation were included in the reference space. For sulfur dioxide, the complete active space in CASSCF consisted of the 2p orbitals of O and the 3p orbitals of S. At the MRCI level, in addition to the 1s orbitals of O, the 2s and 2p orbitals of S were restricted to the frozen core. The 2s orbitals of O, the 3s orbital of S, and the p valence orbitals of S and O were correlated at the MRCI level. Generalized space restrictions were used for the configurations in both O₃ and SO₂. These restrictions restrict the configuration state functions (CSFs) to those having a nonvanishing matrix element with one of the reference configurations.^{54,55} The Davidson correction was applied to the MRCI energies, and these results are denoted as MRCI+Q.⁵⁶

The geometries used can be found in Table 1. For the bent structures the experimental geometries were used.^{3,57} For *cyclic*-O₃ the geometry optimized at the CCSD(T)/cc-pCVQZ level by Müller et al.⁹ was used, while for *cyclic*-SO₂ the geometry optimized at the MRCI/TZ2P level by Kellogg et al. was used.³⁶

The transition state energy from SO₂ to *cyclic*-SO₂ was also found. Geometry optimizations were carried out using an MRCI expansion with the same reference space as above but with only single excitations into the virtual space. The geometry of the conical intersection between the first two ¹A₁ states was optimized using a modified version of COLUMBUS where the algorithm for locating conical intersections was implemented.^{51,58–60} The optimal geometry of the transition state could not be found automatically using the search algorithm available in COLUMBUS, and thus the extremum was found using a grid of points. Forty points between the parameters

TABLE 2: Vertical Excitation Energies of Bent and *cyclic*-O₃ States in C_{2v} Symmetry^a

isomer	state	energy (eV) MRCI ^b	energy (eV) MRCI+Q ^b	oscillator strength ^b	Palmer et al. ^c	Banichevich et al. ^d	Borowski et al. ^e
O ₃	1 ¹ A ₁	0	0		0	0	0
	1 ³ B ₁	1.835	1.733	0	1.8514	1.85	1.62
	1 ³ B ₂	1.709	1.743	0	1.4599	1.69	1.67
	1 ³ A ₂	1.932	1.904	0	2.1520	2.00	1.77
	1 ¹ A ₂	2.122	2.121	0	2.2679	2.16	2.03
	1 ¹ B ₁	2.215	2.149	6.00E-06	2.1516	2.10	2.11
	2 ³ B ₂	4.063	4.043	0	4.3759	3.87	
	2 ¹ A ₁	4.413	4.349	3.00E-06	4.3928	4.49	
	1 ¹ B ₂	5.413	5.185	0.10022	4.8455	5.16	4.69
	2 ³ A ₂	6.107	5.657	0	5.5256	6.01	
				5.9632	5.96		

isomer	state	energy (eV) MRCI ^b	energy (eV) MRCI+Q ^b	oscillator strength ^b
<i>cyclic</i> -O ₃	1 ¹ A ₁ (1 ¹ A ₁ ')	1.367	1.35	
	1 ³ B ₁ (3 ³ E'')	4.861	4.733	0
	1 ³ A ₂ (3 ³ E'')	4.870	4.746	0
	1 ¹ A ₂ (1 ¹ E'')	5.560	5.459	0
	1 ¹ B ₁ (1 ¹ E'')	5.560	5.46	0
	2 ³ B ₁ (3 ³ A ₂ '')	5.740	5.589	0
	2 ³ A ₂ (3 ³ E'')	6.542	6.332	0
	3 ³ B ₁ (3 ³ E'')	6.543	6.335	0
	2 ¹ A ₂ (1 ¹ A ₁ '')	7.266	6.999	0
	3 ¹ A ₂ (1 ¹ E'')	7.269	7.052	0
	2 ¹ B ₁ (1 ¹ E'')	7.275	7.064	0
	3 ¹ B ₁ (1 ¹ A ₂ '')	7.393	7.224	2.00E-06

^a All energies are in eV; the zero energy is taken as the energy of the ground state at bent geometry which is -225.08375 hartrees. ^b This work. ^c Ref 62. ^d Refs 13, 14. ^e Ref 27.

67.500° and 69.500° and between 1.666 and 1.672 Å were used. The points were chosen close to the minimum of the second excited state 2¹A₁ since according to Ivanic et al.²³ the transition state has very similar geometry. The geometry with the gradient vector closest to zero was used to find the energy of the transition state. The single-point energy at the optimal geometry was calculated using an average of states CASSCF and MRCI as described above.

Results and Discussion

I. Ozone and SO₂ Excited States. The vertical excitation energies and the oscillator strengths of O₃ calculated in this work are given in Table 2. In bent O₃, excited electronic states start at 1.7 eV, and the first five excited states are on average 0.1 eV apart from each other. Then there is a gap between the 1¹B₁ and 2³B₂ states, and the rest of the excited states are relatively far apart as compared to the first five. Only the transitions from the ground state 1¹A₁ state to the 2¹A₁, 1¹B₁, and 1¹B₂ states are allowed both by symmetry and multiplicity. Of these, all of the oscillator strengths are small except for the transition of 1¹A₁ → 1¹B₂,^{13,27,61} for which an oscillator strength of 0.100 and a vertical excitation energy of 5.19 eV were calculated. This corresponds to the Hartley band which absorbs in the region between 3000 and 2200 Å²⁷ (4.1–5.6 eV). In addition to the Hartley band, there are three other well-studied diffuse bands. The Chappuis band absorbs in the 6100–5500 Å (1.9–3.1 eV) region and corresponds to the 1¹A₁ → 1¹B₁ transition.^{13,27,61} In this work, a very small oscillator strength of 6×10^{-6} and a vertical excitation energy of 2.15 eV were obtained for this transition. The Huggins band absorbs in the 3740–3000 Å (3.3–4.1 eV) region and is not definitely assigned to a transition thus far. The 2¹A₁ state has a nonzero oscillator strength of 3×10^{-6} . The energy for this transition is 4.35 eV. The Wulf band absorbs in the region 10000–7000 Å (1.1–2.0 eV) and corresponds to the 1¹A₁ → 1¹A₂ (or possibly the 1³A₂)

transition.^{13,27,61} According to our calculations, these states have energies 2.12 and 1.90 eV, respectively. The 1³B₂, 1³B₁, and 1³A₂ states with energies of 1.74, 1.73, and 1.90 eV all fall into the region of the Wulf band in this work.

Vertical excitation energies and oscillator strengths for *cyclic*-O₃ are given in Table 2 also. In this geometry the molecule has D_{3h} symmetry, so both C_{2v} and D_{3h} symmetry labels are given. Some pairs of states that are degenerate in D_{3h} symmetry have energies here that are not exactly degenerate. This is because the references in MRCI were selected to have only the C_{2v} symmetry of the state being calculated. Using this restriction, the size of the calculation was significantly reduced, but the effect of this restriction on the energies was within 0.05 eV for a sample calculation. If all references are included, the states are calculated to be exactly degenerate. The distribution of states of *cyclic*-O₃ is very different from that of bent O₃. In *cyclic*-O₃, the ground and first excited state are separated by 3.38 eV. The next four states in D_{3h} symmetry are separated by 0.53 eV on average. The last three excited states in D_{3h} are very close together, and they correspond to the same electron configuration, (e')¹ × (e'')¹ which gives the A₁''+A₂''+E'' electronic states. The only allowed transition by symmetry for the calculated states in this work is from the ground state to the 1¹A₂'' state. This oscillator strength is very small, 2×10^{-6} .

The vertical excitation energies and oscillator strengths of SO₂ and *cyclic*-SO₂ were also calculated, and the results are shown in Table 3. SO₂ is isovalence to O₃, so similar types of excitations are expected and have been found. Again, the only allowed transitions for bent SO₂ and *cyclic*-SO₂ are from the ground state to any 1¹A₁, 1¹B₁, or 1¹B₂ states. For bent SO₂, the most intense transition has been assigned to the 1¹A₁ → 1¹B₂ transition which absorbs in the region of 2350–1800 Å (5.3–6.9 eV).⁶¹ We obtained a vertical excitation value of 6.49 eV for this transition with an oscillator strength of 0.093. The 1¹A₁ → 1¹B₁ transition corresponds to the band absorbing in

TABLE 3: Vertical Excitation Energies of Bent and cyclic-SO₂ States in C_{2v} Symmetry^a

isomer	state	energy (eV)		energy (eV) MRCI+Q	Palmer et al. ^b
		MRCI	oscillator strength		
SO ₂	1 ¹ A ₁	0		0.000	0
	1 ³ B ₁	3.571	0	3.447	2.94
	1 ¹ B ₁	4.469	0.00691	4.321	3.865
	1 ³ B ₂	4.413	0	4.467	3.635
	1 ³ A ₂	4.546	0	4.555	3.801
	1 ¹ A ₂	4.779	0	4.809	4.165
	1 ¹ B ₂	6.581	0.09262	6.487	5.815
	1 ³ A ₁	7.747	0	7.676	6.648
isomer	state	energy (eV)		energy (eV) MRCI+Q	
		MRCI	oscillator strength		
cyclic-SO ₂	1 ¹ A ₁	4.511		4.465	
	1 ³ A ₂	6.081	0	5.985	
	1 ¹ A ₂	6.752	0	6.660	
	1 ³ B ₁	7.715	0	7.647	
	1 ¹ B ₁	8.078	0.00124	8.033	
	2 ³ B ₁	8.887	0	8.738	
	2 ³ A ₂	9.170	0	8.850	
	1 ³ B ₂	9.930	0	9.824	

^a All energies are in eV; the zero energy is taken as the energy of the ground state at the bent geometry which is -547.907674 hartrees.
^b Ref 46.

the region between 3400 and 2600 Å (3.7–4.8 eV).⁶¹ The vertical excitation value we calculated for this transition is 4.32 eV and the oscillator strength is 0.007. It is well established that the band absorbing in 3900–3400 Å (3.2–3.7 eV) corresponds to the 1¹A₁ → 1³B₁ transition.⁶¹ Our vertical excitation energy of 3.45 eV falls into this region as well.

Unlike O₃, where the first excited state is below 2.0 eV, in SO₂ the energy of the first excited state is at 3.45 eV. The next four excited states are separated by about 0.16 eV similarly to O₃. Then there is a 1.7 eV gap between the 1¹A₂ and 1¹B₂ states. In cyclic-SO₂, the first excited state is at 1.52 eV above the ground. All the states from there on are 0.6 eV apart on average. Again, the energy distributions of the states are very different from each other as geometry changes from the bent to cyclic isomer.

The electronic state energies should be determined as accurately as possible to allow precise development of new laser-based detection schemes for detecting cyclic-O₃. Previously, the CASPT2, MRCI, and DFT methods with various basis sets have been used to calculate the excitation energies of bent O₃.^{11,13,14,27,28,45,62} In this work, the effect of the pVTZ basis set versus the pVQZ basis set on vertical excitation energies was tested using the MRCI method with only single excitations. The difference in vertical excitation energies between the two basis sets was ± 0.015 eV on average. Thus the pVTZ basis set is accurate enough to describe the excited states calculated in this work. The MRCI method is a well-established method for determining the excited states of small molecules, and for this reason it has been selected in this work. Although the MRCI method had been used in the past for the excited states of ozone, it had always been used in conjunction with some selection scheme for the references and configurations. In this work, we include all references and configurations of a given symmetry originating from an active space (12/9), so the previous uncertainties of the selection schemes are removed.

Banichevich et al.^{13,14} used the MRCI method in 1993 to determine the excited states of ozone, but used a smaller basis set and a limited number of configurations than that used in our investigation. They used about 50 references and about 20 000 CSFs. In 2002, Palmer et al. also used the MRCI level

of theory and a similar basis set but they selected the reference space to only a few references.⁶² The effect of their selection of the references on the excitation energies is not clear. As seen in Table 2, the present results agree better with Banichevich than Palmer. Borowski et al. used the CASPT2 method and a similar basis set to obtain vertical excitation energies.²⁷ In this method, the dynamic correlation is estimated with perturbation theory, but the results have been shown to compare well with experimental values. The energies calculated here range from 0.03 to 0.13 eV higher than the Borowski et al. values, except from the energy of the 1¹B₂ state which differs more. The ordering of states they obtained is the same as in our MRCI+Q results. Borowski et al.²⁷ used the same active space as here without any restrictions, while Banichevich et al.¹⁴ and Palmer et al.⁶² used a smaller number of references. The above results indicate that all references should be included for a balanced treatment of all the states.

In the past, the MRCI and DFT methods have been used to calculate the vertical excitation energies of SO₂.^{28,46} Most recently, Palmer et al. used the MRCI method with a pVQZ basis set.⁴⁶ Again, they selected the reference space, and it is unclear what the effects of this selection are on the excitation energies.

Ground-State Energetics. As a further test of the methods used here, the ground state energetics are compared with the ones previously calculated. Much work has been done on the ground-state energy difference between the open and cyclic forms of O₃.^{8–12,16,18,63} Using the MRCI method with a pVQZ basis set and a CASSCF(12/9) reference space, Siebert et al. obtained a value of 1.34 eV (30.9 kcal/mol) for the energy difference.¹⁶ In this study, a value of 1.35 eV (31.1 kcal/mol) was determined using the same method and reference space, but with a pVTZ basis set. Müller et al. calculated the difference to be in the range of 29.1 to 32.2 kcal/mol using the CCSD(T), MRCI, and MR-AQCC levels of theory with correlation consistent basis sets up to the quintuple- ζ quality.⁹ While an experimental value does not exist yet, these theoretical values do compare well with each other.

For SO₂, the energy difference between the ground states of the open and cyclic forms has been calculated here and compared with previous results.^{23,36,37} In 1995, Kellogg et al. used the CCSD(T) method with a triple- ζ basis set and obtained a value of 4.52 eV (104 kcal/mol) for this energy difference.³⁶ Ivanic et al. obtained a value of 97.2 kcal/mol using FORS. We calculated a value of 4.47 eV (103 kcal/mol) for this energy difference. The CCSD(T) and MRCI results are almost identical, and FORS is less than 10 kcal/mol different.

The transition state between the bent and cyclic forms of SO₂ has only been reported at the FORS level by Ivanic et al.²³ This method underestimates the energy difference between bent and cyclic O₃ by 7 kcal/mol compared to the more sophisticated methods. To obtain the energy of the transition state at the more correlated level, it was calculated here using the MRCI wave functions. The transition state from SO₂ to cyclic-SO₂ could not be optimized easily because the transition state, the conical intersection, and the 2¹A₁ minimum are very close to each other on the potential energy surface, and the surface is very steep. Thus a gridpoint was used to find the optimal geometry. The geometry used to find the transition state energy was 67.615° for Θ_{OSO} and 1.666 Å for r_{SO} . The geometry used by Ivanic et al. was 71.4° for Θ_{OSO} and 1.673 Å for r_{SO} . The transition state energy was calculated to be 117 kcal/mol from the C_{2v} minimum. Ivanic et al. obtained a value of 113 kcal/mol for this energy. The geometry for the conical intersection was found

to be $66.015^\circ \Theta_{\text{OSO}}$ and 1.907 \AA for r_{SO} . The same geometry found by Ivanic et al. was 71.0° for Θ_{OSO} and 1.851 \AA for r_{SO} .

II. Electronic Structure Changes from Bent to Cyclic Isomer. The main electron configurations in C_{2v} symmetry of the first and second 1A_1 states and the *cyclic-O₃* ground 1A_1 state are as follows:

$$^1A_1: (5a_1)^2(6a_1)^2(7a_1)^0(1b_1)^2(2b_1)^0(3b_2)^2(4b_2)^2(5b_2)^0(1a_2)^2;$$

$$^2A_1: (5a_1)^2(6a_1)^0(7a_1)^0(1b_1)^2(2b_1)^2(3b_2)^2(4b_2)^2(5b_2)^0(1a_2)^2 + (5a_1)^2(6a_1)^2(7a_1)^0(1b_1)^2(2b_1)^2(3b_2)^2(4b_2)^0(5b_2)^0(1a_2)^2;$$

$$\text{cyclic } ^1A_1: (5a_1)^2(6a_1)^2(7a_1)^0(1b_1)^2(2b_1)^2(3b_2)^2(4b_2)^0(5b_2)^0(1a_2)^2.$$

Only the orbitals in the active space are shown. The electron configuration for the ground state of ozone shown represents 74% of the MRCI wave function. The 2A_1 state has multi-configurational character: the first configuration shown represents 50% of the wave function and the second 36%. The second configuration is formed by the excitation of both $4b_2$ electrons into the $2b_1$ orbital and correlates to the *cyclic-O₃* ground-state configuration in D_{3h} symmetry. The *cyclic-O₃* ground-state configuration shown represents 81% of the MRCI wave function. A conical intersection between the first two 1A_1 states of ozone exists, and thus the 2A_1 state of ozone becomes the *cyclic-O₃* ground state at its minimum. From the single-point calculations of the *cyclic-O₃* excited states, one can see that 2A_1 is so high in energy that it did not appear in our calculations, which have an energy range of 0–7.224 eV from the C_{2v} minimum.

Figure 1 shows the orbitals of O_3 in the active space taken from MCSCF calculations at the bent and cyclic geometries. In the bent O_3 ground state, the active σ (in-plane) $5a_1$, $3b_2$, $6a_1$, and $4b_2$ orbitals and the π (out-of-plane) $1b_1$ and $1a_2$ orbitals are doubly occupied. The excited states are formed by promoting one or two electrons into the empty $2b_1$, $5b_2$, or $7a_1$ orbitals. The lowest excited states calculated in this work are formed mainly from single excitations into the $2b_1$ orbital, except for the 2A_1 , 2^3B_2 , and 2^3A_2 states of O_3 , which are formed by double excitations into the same orbital. Single excitations from the $6a_1$, $1a_2$, and $4b_2$ orbitals form the singlet and triplet $1B_1$, $1B_2$, and $1A_2$ states, respectively. The 2^3B_2 state is formed by excitation of one $6a_1$ electron and one $4b_2$ electron into the $2b_1$ orbital. The second 3A_2 state is formed by the excitations of one $6a_1$ electron and one $1a_2$ electron into the $2b_1$ orbital. One of the configurations of the 2A_1 state corresponds to the *cyclic-O₃* ground state, while the other one is a double excitation from $6a_1$ to $2b_1$. The MRCI wave functions, however, have many other configurations mixed in with the main configuration which contributes between 66% and 85%. The triplet states are lower in energy and less multiconfigurational than their respective singlet states.

cyclic-O₃ has D_{3h} symmetry; therefore several orbitals become degenerate in energy. Figure 1b shows the orbitals in D_{3h} symmetry. The $6a_1$ and $3b_2$ orbitals form an e' orbital, the $7a_1$ and $5b_2$ orbitals form another e' orbital, and the $2b_1$ and $1a_2$ orbitals form an e'' orbital.

In bent O_3 ground state, the $4b_2$ (σ) orbital is doubly occupied. In the *cyclic-O₃* ground state, the $2b_1$ orbital is doubly occupied and the $4b_2$ orbital is empty. In D_{3h} symmetry, the $2b_1$ orbital becomes equal in energy to the $1a_2$; both are lower in energy than the $4b_2$ orbital. Thus, the σ -electrons in the $4b_2$ orbital in bent O_3 become π -electrons in the $2b_1$ orbital in the cyclic isomer. This σ - π transition is the cause of the high barrier to forming *cyclic-O₃*. Using the MRCI wave functions, this transition can be seen.

Because of the orbital degeneracies, some of the *cyclic-O₃* states in this case are degenerate. As seen in Table 2, the 1^3B_1

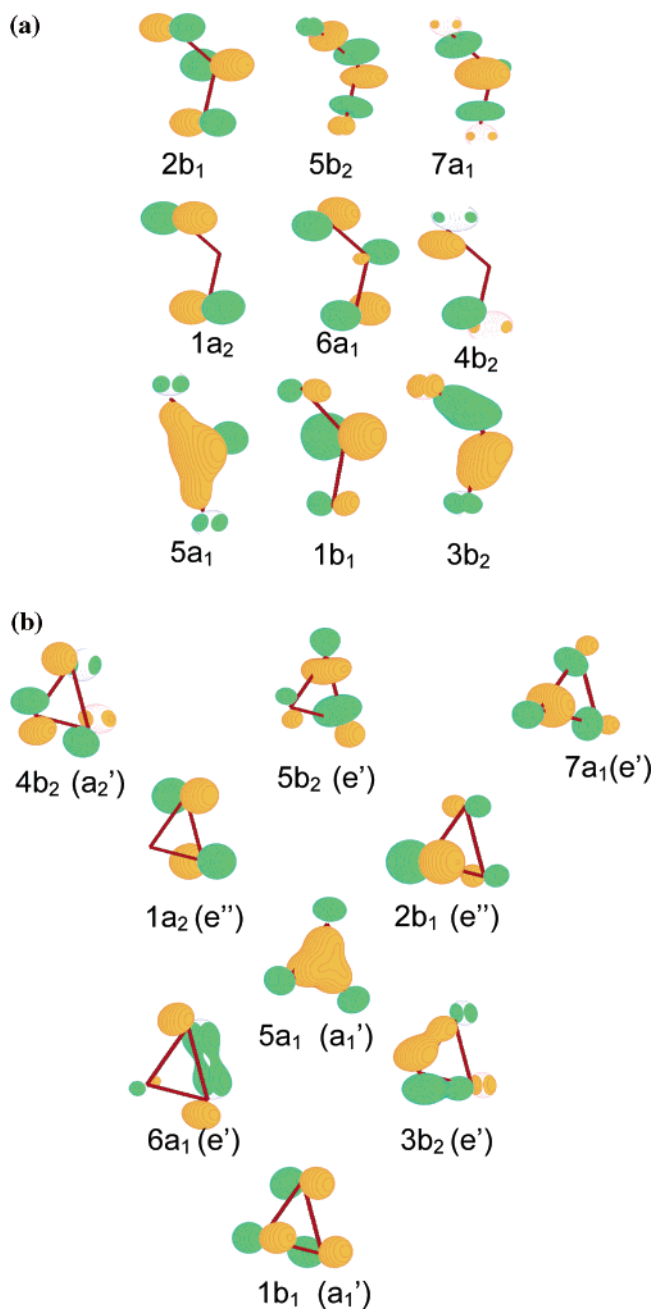


Figure 1. Pictures of the molecular orbitals in the active space for (a) bent O_3 and (b) *cyclic-O₃*. The orbitals are drawn with Molden.⁶⁴ The $2b_1$, $5b_2$, $7a_1$ orbitals are empty in the ground state of bent O_3 .

and 1^3A_2 states are degenerate and become the $1^3E''$ state in D_{3h} . In bent O_3 , these states are 0.17 eV apart. The 1^1A_2 and 1^1B_1 states form the $1^1E''$ state in *cyclic-O₃*; in O_3 , these states are separated by 0.03 eV. The 2^3A_2 state and the 3^3B_1 state together form the $2^3E''$ state. The 3^1A_2 state and the 2^1B_1 state form the $2^1E''$ state.

Excited-state differences in the bent and cyclic structures of ozone are related to the stabilization or destabilization of orbitals when going from one structure to the other. In bent ozone, four excited states are formed by excitations from the $6a_1$ σ -orbital. However, in *cyclic-O₃*, the $6a_1$ orbital is always doubly occupied. Since the $6a_1$ orbital forms the σ -bond between the two outer oxygen atoms in the cyclic isomer, this orbital is stabilized in the cyclic geometry, and electrons are not excited from it. In bent O_3 , the $7a_1$ and $5b_2$ orbitals are high in energy and always empty. However in *cyclic-O₃*, the last five excited states in D_{3h}

calculated in this work are formed by single excitations from one of the *cyclic*-O₃ ground-state orbitals to the 7a₁ or 5b₂ orbitals (which together form an e'). All of the states formed by this excitation are higher in energy than the calculated excited states of bent ozone with the exception of the bent 2³A₂ state, which is slightly higher in energy than the cyclic 2³B₁ state.

For bent O₃, the 2¹A₁ state correlates to the cyclic ground state. Also the 1¹A₂ and 1³A₂ states correlate to the *cyclic*-O₃ 1¹A₂ and 1³A₂ states. In these states, the 4b₂ and 2b₁ orbitals are singly occupied. While in bent O₃ the electron was excited from the 4b₂ into the 2b₁, in *cyclic*-O₃ the electron is excited from the 2b₁ into the 4b₂. These are the only three states that correlate between the two isomers. All other states differ in configuration because of the orbital energy differences between the bent and cyclic geometry.

In SO₂, the valence orbitals are now the σ 7a₁, 4b₂, 8a₁, and 5b₂ orbitals and the π 2b₁ and 1a₂ orbitals. For bent SO₂, the 2¹A₁ state was so high in energy that it did not appear in this calculation. However, we expect that this state correlates with the *cyclic*-SO₂ ground state. The 1¹A₂ and 1³A₂ states of the bent structure also correlate to the cyclic 1¹A₂ and 1³A₂ states and have the same valence orbital configurations as those for bent and *cyclic*-O₃. The 1³B₂ states of the bent and *cyclic*-SO₂ isomers also correlate. In bent SO₂, this state corresponds to a single excitation from the 1a₂ orbital to the 3b₁ orbital. For *cyclic*-SO₂, this state corresponds to a double excitation in which one electron is excited from each of the 1a₂ and 3b₁ orbitals into the 4b₂ orbital. This may explain why the 1³B₂ state is so much higher in energy for the cyclic isomer relative to the bent isomer. All other states do not correlate with states at energies that have not been calculated.

The excited states of SO₂ have character similar to those of O₃, but the energies differ considerably. The O–SO bond strength is much stronger than the O–OO bond strength, and therefore, SO₂ is much more stable in its ground state form than O₃. Thus in SO₂, the excited states are much higher in energy from the ground state. However, in *cyclic*-O₃ and *cyclic*-SO₂, the opposite is true. The excited states of *cyclic*-O₃ are higher in energy from the cyclic minimum than the *cyclic*-SO₂ excited states are from the cyclic minimum.

III. Detection and CARS. An essential step in the synthesis of *cyclic*-O₃ concerns detection of this molecule in the presence of O₂ and ozone. CARS is under investigation as a method to detect *cyclic*-O₃. In the CARS technique, knowledge of the excited-state structure is essential. To use CARS, a pump laser beam (ω_1) excites the molecule to a virtual state. A second Stokes beam (ω_2) is tuned such that the energy difference between the pump and Stokes beams equals the energy difference between two eigenstates of the molecule to be detected. Coherent excitation through the virtual state allows the Stokes beam to populate a real eigenstate of the molecule. A second pump beam (ω_1) then excites the molecule from the real excited state to a second virtual state. The CARS signal of frequency $\omega_{\text{CARS}} = 2\omega_1 - \omega_2$ will be generated as a fourth coherent laserlike beam (ω_{CARS}) whose frequency is given by the conservation of energy and whose direction is given by conservation of momentum. To avoid populating an excited electronic state of the molecule (rather than a virtual state), the excited states of the target molecule must be known. The excited electronic states reported in Tables 2 and 3 and the vibrational states in Table 4 provide the information necessary to determine the pumping scheme. The vibrational levels for O₃ and *cyclic*-O₃ are taken from Siebert et al.,^{16,26} the vibrational levels of

TABLE 4: Vibrational Energies (cm⁻¹)

isomer	mode	energy	isomer	mode	energy
O ₃ ^a	v ₁	1101.9	SO ₂ ^c	v ₁	1152
	v ₂	698.5		v ₂	518
	v ₃	1043.9		v ₃	1362
<i>cyclic</i> -O ₃ ^b	v ₁	1099.6	<i>cyclic</i> -SO ₂ ^d	v ₁	1088
	v ₂ = v ₃	782.9		v ₂	739
				v ₃	805

^a Ref 16. ^b Ref 26. ^c Ref 57. ^d Ref 37.

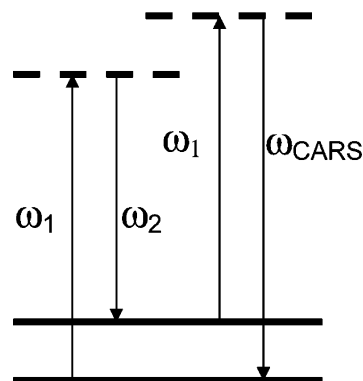


Figure 2. Energy diagram for Coherent Anti-Stokes Raman Spectroscopy (CARS). Arrows represent laser beams of frequency ω . Solid black lines are vibrational levels of the molecule. Dashed lines are virtual states of the molecule.

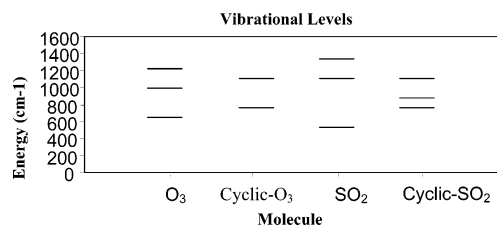


Figure 3. The vibrational states of O₃, *cyclic*-O₃, SO₂, *cyclic*-SO₂ taken from Table 4 references.

SO₂ and *cyclic*-SO₂ are taken from Rassias et al. and Chen et al., respectively.^{37,57}

CARS is anticipated to be an excellent method for discriminating between the cyclic and open forms of ozone (Figure 2). Even trace amounts of a sample can be detected using CARS because the signal is created in a coherent laserlike emission beam that can be separated from incoherent noise and easily collected in full. The vibrational energy levels for the ground state of ozone and O₂ have been both previously calculated and measured. The vibrational levels for *cyclic*-O₃ have been calculated previously, as well. As seen in Table 4 and Figure 3, the vibrational transition energies in the two isomers are quite different, suggesting that a vibrational spectroscopic technique such as CARS should discriminate between the two isomers. If the wavelength of the laser is tuned to search for the v₂ mode of *cyclic*-O₃, then the mode of ozone that is closest in energy is also the v₂ mode, and the two are separated by 84.4 cm⁻¹. This places a restriction on the bandwidth of the excitation pulses.

The calculated electronic states for O₃, *cyclic*-O₃, SO₂, and *cyclic*-SO₂ can be used to determine the optimal CARS detection scheme for each reactant product pair. Because of the current laser technology, 800 nm is a convenient wavelength to use for the pump photon. As seen in Figure 4b, a one- or two-800-nm photon scheme can be used to detect *cyclic*-O₃ because of the large energy spacing between the ground state of *cyclic*-O₃ and its excited states. Similar diagrams are shown for the other three molecules in Figure 4a,c,d. For bent ozone, the calculations

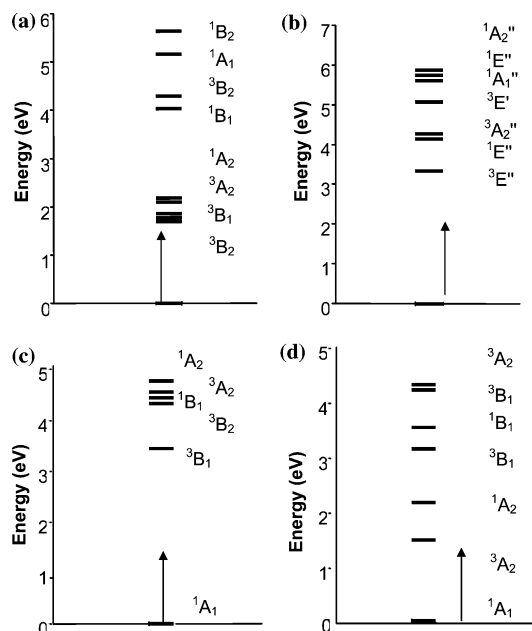


Figure 4. CARS Scheme for detection of a molecule using calculated eigenstate energies at the MRCI+Q level. Arrows represent 800-nm photons, and black lines mark electronic states. Energy is in eV on the y-axis. (a) Scheme for O_3 , (b) scheme for *cyclic*- O_3 , (c) scheme for SO_2 , (d) scheme for *cyclic*- SO_2 .

suggest that a one- or two-800-nm photon scheme is appropriate because of the gap between the ground and first excited states and the large gap between the fifth and sixth excited states. For SO_2 , a one- or two-800-nm photon scheme is also possible because of the large energy space between the ground and first excited state. Last, the calculations for *cyclic*- SO_2 suggest that a one-800-nm photon scheme is preferable because the energy gap between the ground and first excited state is only 1.52 eV.

Conclusions

The energies of the ground and first eleven excited states for *cyclic*- O_3 and the ground and first seven excited states for *cyclic*- SO_2 have been calculated and compared with the excited states at the observed minima of these molecules. These were calculated using large MRCI expansions of about 40 million CSFs per C_{2v} symmetry and a cc-pVTZ basis set. The excited-state distributions and character at the cyclic structure differ from those at the bent structure. The energy difference between the bent and cyclic minima was calculated to be 103 kcal/mol for SO_2 and 31.1 kcal/mol for O_3 , in agreement with previous calculations. The transition state geometry for ring closing of SO_2 was found to be $\Theta_{OSO} = 67.615^\circ$ and $r_{SO} = 1.666 \text{ \AA}$. The energy at this point was calculated to be 117 kcal/mol from the C_{2v} minimum. We have found that it is possible to use a one-photon CARS scheme to detect the formation of *cyclic*- O_3 and *cyclic*- SO_2 because of the vibrational and electronic state spacings. This work represents the first step in our efforts to synthesize *cyclic*- O_3 and *cyclic*- SO_2 .

Acknowledgment. The authors acknowledge the generous support of the Air Force Office of Scientific Research, and DARPA and the National Science Foundation (R.J.L. Grant No. CHE-313967 and S.M. Grant No. CHE-0449853). We also thank David Dalton for stimulating discussions, particularly with regard to comparisons to SO_2 .

References and Notes

- (1) Meyer, L. *Modern Theories of Chemistry*; Longmans: London, 1888.
- (2) Herzberg, G. *Electronic Structure of Polyatomic Molecules*; Van Nostrand: Princeton, 1967.
- (3) Tanaka, T.; Morino, Y. *J. Mol. Spectrosc.* **1970**, *33*, 538.
- (4) Plass, R.; Egan, K.; Collazo-Davila, C.; Grozea, D.; Landree, E.; Marks, L.; Gajdardziska-Josifovska, M. *Phys. Rev. Lett.* **1998**, *81*.
- (5) Lo, W.-J.; Wu, Y.-J.; Lee, Y.-P. *J. Chem. Phys.* **2002**, *117*, 6655.
- (6) Lo, W.-J.; Wu, Y.-J.; Lee, Y.-P. *J. Phys. Chem. A* **2003**, *107*, 6944.
- (7) Peyerimhoff, S. D.; Buenker, R. J. *J. Chem. Phys.* **1967**, *47*, 1953.
- (8) Shih, S.; Buenker, R.; Peyerimhoff, S. *Chem. Phys. Lett.* **1974**, *28*.
- (9) Muller, T.; Xantheas, S.; Dachsel, H.; Harrison, R.; Nieplocha, J.; Shepard, R.; Kedziora, G.; Lischka, H. *Chem. Phys. Lett.* **1998**, *293*, 72.
- (10) Lee, T. *J. Chem. Phys. Lett.* **1990**, *169*, 529.
- (11) Hay, P.; Dunning, T. *J. Chem. Phys.* **1997**, *67*.
- (12) Harding, L.; Goddard, W. *J. Chem. Phys.* **1997**, *67*.
- (13) Banichevich, A.; Peyerimhoff, S. *Chem. Phys.* **1993**, *174*, 93.
- (14) Banichevich, A.; Peyerimhoff, S.; Grein, F. *Chem. Phys.* **1993**, *178*, 155.
- (15) Atchity, G.; Ruedenberg, K. *Theor. Chem. Acc.* **1997**, *96*, 176.
- (16) Siebert, R.; Fleurat-Lessard, P.; Schinke, R. *J. Chem. Phys.* **2002**, *116*.
- (17) Tyuterev, V. G.; Tashkun, S.; Jensen, P.; Barbe, A.; Cours, T. *J. Mol. Spectrosc.* **1999**, *198*, 57.
- (18) Xantheas, S.; Atchity, G.; Elbert, S.; Ruedenberg, K. *J. Chem. Phys.* **1991**, *94*, 8054.
- (19) Yamashita, K.; Morokuma, K.; Le Quere, F.; Leforestier, C. *Chem. Phys. Lett.* **1992**, *191*, 515.
- (20) Siebert, R.; Schinke, R.; Bittererova, M. *PCCP Commun.* **2001**, *3*, 1795.
- (21) Xie, D.; Guo, H.; Peterson, K. A. *J. Chem. Phys.* **2000**, *112*, 8378.
- (22) NSRSR-NBS. JANAF Thermochemical Tables; US GPO: Washington, DC, 1971.
- (23) Ivanic, J.; Atchity, G. J.; Ruedenberg, K. *J. Chem. Phys.* **1997**, *107*, 4307.
- (24) Flemmig, B.; Wolczanski, P.; Hoffmann, R. *J. Am. Chem. Soc.* **2005**, *127*, 1278.
- (25) Artamonov, M.; Ho, T.; Rabitz, H. *Chem. Phys.* **2004**, *305*, 213.
- (26) Siebert, R.; Schinke, R. *J. Chem. Phys.* **2003**, *119*.
- (27) Borowski, P.; Fulscher, M.; Malmqvist, P.; Roos, B. *Chem. Phys. Lett.* **1995**, *237*, 195.
- (28) Jones, R. O. *J. Chem. Phys.* **1985**, *82*, 325.
- (29) Myerson, A. L.; Taylor, F. R.; Hanst, P. L. *J. Phys. Chem.* **1957**, *26*, 1309.
- (30) Norrish, R. G. W.; Zeelenberg, A. P. *Proc. R. Soc. London, Ser. A* **1957**, *240*.
- (31) Norrish, R. G. W.; Oldershaw, G. A. *Proc. R. Soc. London, Ser. A* **1959**, *249*, 498.
- (32) Levy, A.; Merryman, E. L. *Environ. Sci. Technol.* **1969**, *3*, 63.
- (33) McGarvey, J. J.; McGrath, W. D. *Proc. R. Soc. London, Ser. A* **1964**, *278*, 490.
- (34) Hayes, E. F.; Pfeiffer, G. V. *J. Am. Chem. Soc.* **1968**, *90*, 4773.
- (35) Dunning, T. H.; Raffanetti, R. *J. Phys. Chem.* **1981**, *85*, 1350.
- (36) Kellogg, C. B.; Schaefer, H. F., III. *J. Phys. Chem.* **1995**, *99*, 4177.
- (37) Chen, L.; Lee, C.; Lee, Y. *J. Chem. Phys.* **1996**, *105*, 9454.
- (38) Morino, Y.; Kikuchi, Y.; Saito, S.; Hirota, E. *J. Mol. Spectrosc.* **1964**, *13*, 95.
- (39) Xie, D. Q.; Guo, H.; Bludsky, O.; Nachtigall, P. *Chem. Phys. Lett.* **2000**, *329*, 503.
- (40) Xu, D. G.; Lu, Y. H.; Xie, D. Q.; Yan, G. S. *Chem. J. Chin. University* **2000**, *21*, 1884.
- (41) Zheng, Y. J.; Ding, S. L. *Acta Chim. Sin.* **2000**, *58*, 56.
- (42) Zuniga, J.; Bastida, A.; Requena, A. *J. Chem. Phys.* **2001**, *115*, 139.
- (43) Rodrigues, S. P. J.; Sabin, J. A.; Varandas, A. J. C. *J. Phys. Chem. A* **2002**, *106*, 556.
- (44) Ma, G. B.; Chen, R. Q.; Guo, H. *J. Chem. Phys.* **1999**, *110*, 8408.
- (45) Kamiya, K.; Matsui, H. *Bull. Chem. Soc. Jpn.* **1991**, *64*, 2792.
- (46) Palmer, M.; Shaw, D.; Guest, M. *Mol. Phys.* **2005**, *103*, 1183.
- (47) Norwood, K.; Ng, C. Y. *J. Chem. Phys.* **1990**, *92*, 1513.
- (48) Bendazzoli, G. L.; Palmerieri, P. *Int. J. Quantum Chem.* **1975**, *9*, 537.
- (49) Levis, R. J.; Menkir, G. M.; Rabitz, H. *Science* **2001**, *292*, 709.
- (50) Levis, R. J.; Rabitz, H. A. *J. Phys. Chem.* **2002**, *106*, 6427.
- (51) Lischka, H.; Shepard, R.; Pitzer, R. M.; Shavitt, I.; Dallos, M.; Muller, T.; Szalay, P. G.; Seth, M.; Kedziora, G. S.; Yabushita, S.; Zhang, Z. Y. *Phys. Chem. Chem. Phys.* **2001**, *3*, 664.
- (52) Dunning, T. H. *J. Chem. Phys.* **1989**, *90*, 1007.
- (53) Woon, D. E.; Dunning, T. H. *J. Chem. Phys.* **1993**, *98*, 1358.
- (54) Bunge, A. *J. Chem. Phys.* **1970**, *53*, 20.

- (55) McLean, A.; Liu, B. *J. Chem. Phys.* **1973**, *58*, 1066.
- (56) Langhoff, S. R.; Davidson, E. R. *Int. J. Quantum Chem.* **1974**, *8*, 61.
- (57) Rassias, G.; Metha, G.; McGilvery, D.; Morrison, R.; O'Dwyer, M. *J. Mol. Spectrosc.* **1997**, *181*, 78.
- (58) Lischka, H.; Dallos, M.; Shepard, R. *Mol. Phys.* **2002**, *100*, 1647.
- (59) Lischka, H.; Dallos, M.; Szalay, P. G.; Yarkony, D. R.; Shepard, R. *J. Chem. Phys.* **2004**, *120*, 7322.
- (60) Dallos, M.; Lischka, H.; Shepard, R.; Yarkony, D. R.; Szalay, P. *J. Chem. Phys.* **2004**, *120*, 7330.
- (61) Herzberg, G. *Molecular Spectra and Molecular Structure*; Van Nostrand: New York, 1966; Vol. 3.
- (62) Palmer, M.; Nelson, A. *Mol. Phys.* **2002**, *100*, 3601.
- (63) Burton, P. *J. Chem. Phys.* **1979**, *71*.
- (64) Schaftermaar, G.; Noordik, J. *J. Comput.-Aided Mol. Des.* **2000**, *14*, 123.